Nonadiabatic effects induced by the coupling between vibrational modes via Raman fields

Vishesha Patel and Svetlana Malinovskaya
Department of Physics and Engineering Physics, Stevens Institute of Technology, Hoboken, New Jersey 07030, USA
(Received 16 November 2010; published 31 January 2011)

We study the effect of coupling between molecular vibrational modes attendant the excitation of Raman transitions using ultrafast chirped laser pulses. We model Raman-active vibrational modes by two-level systems (TLSs) with nondegenerate ground states and a predetermined initial relative phase. Chirp of the pump and Stokes pulses is the same in magnitude and opposite in sign for the whole pulse duration. To reveal the nonadiabatic effects induced by the coupling between the vibrational modes, we compare the model of two uncoupled TLSs with the one of two TLSs coupled by the external fields. The first model shows population inversion. Within the second model, the coupling induces nonadiabatic effects leading to a mixed population distribution. By introducing the time delay between the Stokes and pump pulses, nearly complete population transfer is realized in both coupled TLSs.

DOI: 10.1103/PhysRevA.83.013413 PACS number(s): 32.80.Xx, 33.80.Be, 42.50.−p, 33.20.Tp

I. INTRODUCTION

Advances in laser technology hold a treasure for controlled optical excitations in atoms and molecules. In a simplistic picture, any transitions in a molecule may be described by a model of a multilevel system interacting with light and, often, by a two-level system (TLS) [1]. In the resonantly driven TLS, it is possible to obtain the desired population transfer by applying a driving pulse that provides a specific value of the pulse area. The population inversion takes place when the pulse is in resonance with the TLS and satisfies the condition that the pulse area is equal to π. However, in real molecular systems, existence of multiple transitions with various coupling strengths and frequencies makes it impossible to use the pulse area solution to achieve a predetermined population transfer (e.g., population inversion). One is likely to find the inversion in one transition and a complete population return in another transition, as well as arbitrary population distribution in other transitions. Another drawback of the π-pulse method is that it requires precise control over the pulse area. Besides, certain constraints have to be imposed on a system of interest; for example, the orientation of the transition dipoles related to the impinging field. All of these restricts the application of the π-pulse approach to specific molecular systems only.

For a molecular system characterized by a vibrational spectrum composed of very close transition frequencies, the problem of robust population inversion is a big challenge. Various quantum control techniques, however, demonstrated successful generating of ultrafast amplitude- or phase-modulated laser pulses that steer a molecular system to the desired quantum yield. One of the most interesting features of these optically modulated pulses is the chirp. Chirping the pulse causes temporal variation of the carrier frequency. It has become evident that positively and negatively chirped laser pulses are crucial for achieving population inversion. Malinovsky *et al.* [2] and Cao *et al.* [3] suggested a population inversion scheme based on positively chirped pulses in TLSs. Upon application of ultrafast chirped laser pulses, population inversion was demonstrated by Bergmann *et al.* [4] in a three-level system and in the case of a more complex multilevel system by Kobrak and Rice [5] and also by Moon *et al.* [6]. Using linearly chirped picosecond pulses, Amstrup and coworkers [7] demonstrated the feasibility of adiabatic inversion in I_2 vapor. Meanwhile, Ruhman and Kosloff [8] showed that negatively chirped pulses are more efficient than their unchirped counterparts. Following this study, Cerullo *et al.* [9] observed strong chirp dependence for high-power femtosecond pulse excitation of dye molecules in solution and found that the process is enhanced by negatively chirped pulses and suppressed by positively chirped pulses.

Adiabatic passage is known to involve a dynamic variable (for example, the field amplitude or field-state detuning) which changes sufficiently slowly compared to other time-dependent parameters of the light-matter system. The evolution of states in this case is subject to an effective Hamiltonian. Adiabatic passage may be accomplished when an atom or a molecule remains in a single eigenstate (the dressed state) of that effective Hamiltonian at all times. It has been efficiently used to adiabatically invert population starting from the pure initial state. This task is of key importance in experimental and theoretical work addressing problems in quantum computing, atomic and molecular spectroscopy, etc.

In this article, a semiclassical theory is developed to study the interaction of the Raman-active vibrational modes, described by TLSs, with femtosecond chirped laser pulses. An exact solution is obtained by numerically solving the time-dependent Schrödinger equation using the Runge-Kutta method. The primary goal is to reveal the nonadiabatic effects induced by the coupling between the vibrational modes. Two cases are considered: first, when two Raman-active vibrational modes are uncoupled while interacting with external fields and, second, when they are coupled via an external field. The coupling leads to a nonzero probability of population transfer from one TLS to another via the pump and Stokes pulses. Further, the dressed-state analysis is carried out to compare the adiabatic approximation with the exact solution obtained from the Schrödinger equation and to reveal the strength of the nonadiabatic effects induced by the coupling. Finally, the time delay between the pump and Stokes pulses is introduced as a tool to compensate for the nonadiabatic effects and to achieve a complete population transfer in both coupled vibrational modes.

II. THEORY

A semiclassical theory is developed that describes the interaction of femtosecond chirped laser pulses with two TLSs representing two Raman-active vibrational modes in a molecule. Relaxation or collisional dephasing effects are not taken into account. Two TLSs have nondegenerate energies of the ground states, as shown in Fig. 1. The energy levels of each TLS are chosen in accordance with the solution for a one-dimensional harmonic oscillator. Here the $|1\rangle$-$|2\rangle$ TLS has transitional frequency ω_{21} and the $|3\rangle$-$|4\rangle$ TLS has transitional frequency ω_{43} such that $\omega_{43} - \omega_{21} = \delta$. Our prime interest is to learn how the coupling between TLSs impacts the population dynamics and if it is possible to achieve a population inversion in both the $|1\rangle$-$|2\rangle$ and $|3\rangle$-$|4\rangle$ TLSs when they are coupled through the fields.

The femtosecond pump and Stokes laser pulses have Gaussian envelopes and are linearly chirped. They have carrier frequencies ω_p and ω_s respectively, and are defined as

$$E_p(t) = E_{p0}(t)\cos\left(\omega_p t - \frac{\alpha t^2}{2}\right),$$
$$E_s(t) = E_{s0}(t)\cos\left(\omega_s t - \frac{\beta t^2}{2}\right), \quad (1)$$
$$E_{p0}(t) = E_{p0}e^{-\frac{t^2}{2\tau^2}}, \quad E_{s0}(t) = E_{s0}e^{-\frac{t^2}{2\tau^2}},$$

where $E_{p0}(t)$ and $E_{s0}(t)$ are the time-dependent pump and Stokes field envelopes, $E_{p0} = E_0/(1+\frac{\alpha'^2}{\tau_0^4})^{1/4}$ is the peak value of the pump pulse, $E_{s0} = E_0/(1+\frac{\beta'^2}{\tau_0^4})^{1/4}$ is the peak value of the Stokes pulse, α, β and α', β' are the linear temporal and respective spectral chirps of the pump and Stokes pulse, $\tau = \tau_0\sqrt{1+\alpha'^2/\tau_0^4}$ is the chirp-dependent pulse duration assumed to be the same for the pump and Stokes pulses since $|\alpha'| = |\beta'|$, (pulse chirping is known to elongate the pulse duration). Let us look first at the case when two TLSs interact with the pump and Stokes fields without interacting with each other, which means that the TLSs are uncoupled. Within the field-interaction representation, a semiclassical Hamiltonian that describes the interaction of each of two uncoupled TLSs with ultrafast chirped laser pulses reads

$$H = \begin{pmatrix} -\delta/2 - \alpha_d(t)/2 - \Omega_d(t) & -\Omega_3(t) \\ -\Omega_3(t) & \delta/2 + \alpha_d(t)/2 + \Omega_d(t) \end{pmatrix}. \quad (2)$$

It is obtained by adiabatic elimination of the virtual electronic excited state $|b\rangle$ and in the rotating-wave approximation (RWA). Here, the two-photon detuning δ is zero for the resonant TLS. When the coupling between the resonant and detuned TLS is switched on, the Hamiltonian for the coupled TLSs, obtained in the field-interaction representation and the RWA after adiabatic elimination of the virtual state $|b\rangle$, reads

$$H = \begin{pmatrix} -\alpha_d(t) - \Omega_d(t) & -\Omega_3(t) & -\Omega_1(t) & -\Omega_3(t) \\ -\Omega_3(t) & \alpha_d(t) + \Omega_d(t) & -\Omega_3(t) & -\Omega_2(t) \\ -\Omega_1(t) & -\Omega_3(t) & \delta/2 - \alpha_d(t) - \Omega_d(t) & -\Omega_3(t) \\ -\Omega_3(t) & -\Omega_2(t) & -\Omega_3(t) & 3\delta/2 + \alpha_d(t) + \Omega_d(t) \end{pmatrix}, \quad (3)$$

Here $\Omega_d(t) = [\Omega_1(t) - \Omega_2(t)]/2$, $\alpha_d(t) = (\beta - \alpha)(t - t_c)$, $\Omega_1(t) = \frac{\mu^2}{4\hbar^2\Delta}E_{p0}^2\exp[-\frac{(t-t_c)^2}{\tau^2}]$, $\Omega_2(t) = \frac{\mu^2}{4\hbar^2\Delta}E_{s0}^2\exp[-\frac{(t-t_c)^2}{\tau^2}]$ are the ac Stark shifts originated from the two-photon transition, t_c is the central time when the pump and Stokes pulse amplitude comes to the peak value, μ is the dipole moment (for simplicity we considered all the dipole moments to be equal to 1 Debye; $\mu_{ij} = \mu$), Δ is the detuning from the electronic excited state $|b\rangle$, and $\Omega_3(t) = \frac{\mu^2}{4\hbar^2\Delta}E_{p0}E_{s0}\exp[-\frac{(t-t_c)^2}{\tau^2}]$ is the effective Rabi frequency. The diagonal elements of the Hamiltonian describe bare-state energies in the field-interaction representation; they depend on the chirp parameters α and β and also on detuning δ. The off-diagonal elements represent coupling of the bare states through the effective Rabi frequency $\Omega_3(t)$ and also through the ac Stark shifts.

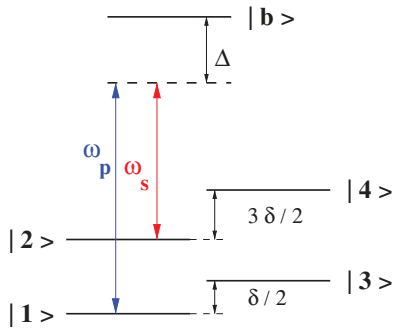

FIG. 1. (Color online) Schematic of two TLSs having frequencies ω_{21} and ω_{43}. Ground states are equally populated initially. The vibrational modes interact with the pump and Stokes pulses having frequencies ω_p and ω_s respectively, and Δ is the one-photon detuning from the excited state $|b\rangle$.

III. NUMERICAL RESULTS FOR THE MODEL OF TWO UNCOUPLED TWO-LEVEL SYSTEMS

The Hamiltonian in Eq. (2) is used in the Schrödinger equation to solve for the evolution of the probability amplitudes $a_1(t)$ and $a_2(t)$ for the resonant TLS and for the probability amplitudes $a_3(t)$ and $a_4(t)$ for the detuned TLS (see Fig. 1). The numerical solution was obtained using the Runge-Kutta method [10] and performed under the initial condition that

only the ground state of the resonant TLS and the detuned TLS is populated. This is likely to be the case for population distribution in molecules at room temperature. The population is chosen to be 0.5, so the total population in two TLSs is unity. If two TLSs are uncoupled, a single state population can reach the maximum value of 0.5; however, if two TLSs are coupled (for details see the next section) a single state population can range from zero to 1. The parameters of the fields and the systems used in numerical calculations correlate with experimental conditions discussed in [11,12] and also used in [13]. We addressed two Raman-active vibrational modes $\omega_{21} = 84.9$ THz (2840 cm^{-1}), the symmetric stretch, and $\omega_{43} = 87.6$ THz (2930 cm^{-1}), the asymmetric stretch, in methanol. (They are an equally good fit for vibrational modes of the CH_n molecular species, found in abundance in biological samples [14].) The intensity of the laser fields is 2×10^{12} W/cm^2, and the transform-limited pulse duration is $\tau_0 = 176$ fs. The magnitude of the spectral chirp used in calculations is fixed and is $|\alpha'| = |\beta'| = 3 \times 10^{-4}$/cm^{-2}, giving the chirped pulse duration equal to $\tau = 1.8$ ps. Under the condition of the same magnitude of the chirp for both the pump and Stokes pulses, the chirp rate is positive for the pump pulse ($\alpha > 0$) and negative for the Stokes pulse ($\beta < 0$). Besides, at the instant t_c when the pump- and Stokes-pulse amplitudes reach their peak value, the frequency difference $(\omega_p - \omega_s)$ comes into resonance with the transitional frequency ω_{21}. The resonance with the ω_{43} transitional frequency is achieved somewhat later, at $t = t_c + \delta/(2\alpha)$, (where α is the positive chirp parameter of the pump pulse). The detuning δ, that features the $|3\rangle$-$|4\rangle$ TLS, is much less than the transition frequency of the resonant TLS (i.e., $\delta \ll \omega_{21}$), and is equal to 2.7 THz in our calculations. Figure 2 shows the population dynamics in the resonant TLS. The population is being smoothly transferred from the ground state to the excited state, the even population distribution is achieved at the central time and the inversion occurs at the end of the pulse duration. In Fig. 3, the population dynamics in the detuned TLS is shown. In this case, the even population distribution is achieved

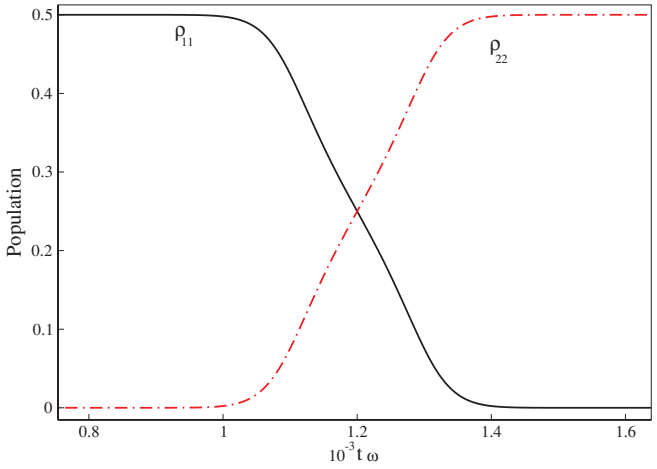

FIG. 2. (Color online) The population dynamics in the resonant TLS as a function of time for parameters $\alpha'/\tau_0^2 = 10$ and the peak pulse intensity 2×10^{12} W/cm^2. The black (solid) and red (dot-dashed) curves show the exact solution for population in states $|1\rangle$ and $|2\rangle$, respectively.

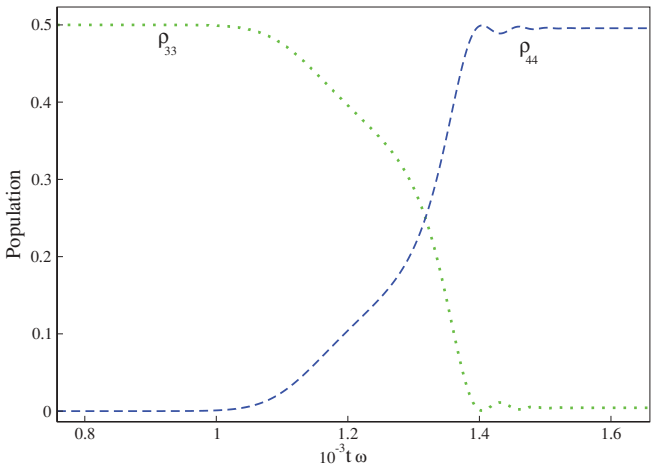

FIG. 3. (Color online) The population dynamics in the detuned TLS as a function of time for parameters $\alpha'/\tau_0^2 = 10$ and the peak pulse intensity 2×10^{12} W/cm^2. The green (dotted) and blue (dashed) curves show the exact solution for populations in states $|3\rangle$ and $|4\rangle$, respectively.

at time $t = t_c + \delta/(2\alpha)$ and the population inversion takes place at the end of the pulse. Simultaneously applied, the negatively chirped Stokes pulse and the positively chirped pump pulse compose the field having the beat frequency continuously changing from a lower to higher value. Since frequency difference of the detuned TLS is $\omega_{21} + \delta$, the field beat frequency comes into resonance with this TLS after the central time, so inversion in the $|3\rangle$-$|4\rangle$ TLS occurs later than in the $|1\rangle$-$|2\rangle$ TLS.

To gain an insight into the adiabaticity of the population transfer, the dressed-state analysis was carried out. We numerically diagonalized the Hamiltonian in Eq. (2) and obtained the time-dependent energy of the dressed states and their respective eigenvectors. Figure 4 shows the dressed -state energies (solid lines) and the bare-state energies (dashed lines) as a function of time for the resonant TLS. Dressed state I is populated initially because it coincides with the bare state $|1\rangle$,

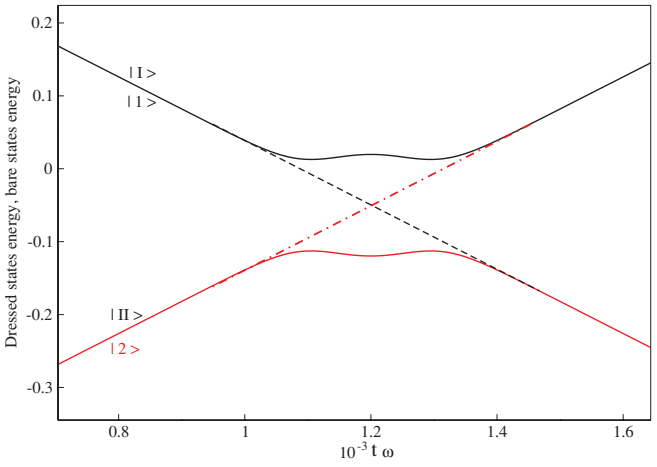

FIG. 4. (Color online) Time-dependent picture of the energies of the dressed states I and II (solid lines) and the energies of the bare states (dashed lines) for the resonant TLS as a function of time for parameters $\alpha'/\tau_0^2 = 10$ and a peak pulse intensity 2×10^{12} W/cm^2.

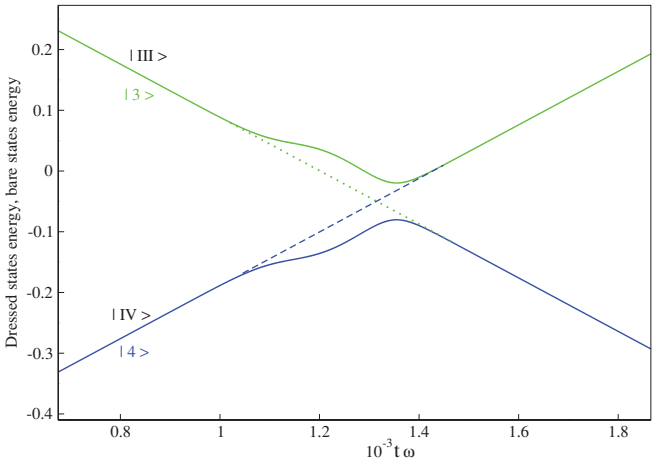

FIG. 5. (Color online) Time-dependent picture of the energies of the dressed states III and IV (solid lines) and the energies of the bare states (dashed lines) for the detuned TLS as a function of time for parameters $\alpha'/\tau_0^2 = 10$ and a peak pulse intensity 2×10^{12} W/cm^2.

which is the ground state of the resonant TLS. Thus, dressed state I is the state within which the adiabatic dynamics takes place. As the pulses evolve in time and the intensity of the fields increases, this dressed state becomes a superposition of two bare states with the same probability amplitude. Asymptotically, the energy of dressed state I coincides with the energy of bare state $|2\rangle$, manifesting the population inversion. The plots for the dressed-state energies of the detuned TLS are shown in Fig. 5; they are labeled III and IV. Note that here the crossing of the bare states occurs after the central time because of the detuning in the system. At the end of the pulse duration, almost complete population inversion is observed in this TLS as well.

Figure 6 shows the population distribution among the bare states obtained from the eigenvectors related to dressed states I, II, III, and IV. The population of the bare states within dressed state I shows an adiabatic transfer of all the population from state $|1\rangle$ to state $|2\rangle$. However, the reverse is observed for dressed state II's population dynamics. For dressed state III, plots depict an inversion from bare state $|3\rangle$ to bare state $|4\rangle$ and, for dressed state IV, the population dynamics are reversed compared to dressed state III. The crossings of the bare-state populations are consistent with Figs. 4 and 5 and occur after the central time for the detuned TLS and at the central time for the resonant TLS. Thus, we have demonstrated that an adiabatic control leading to the population inversion is possible in a resonant or slightly detuned TLS by implementing the same in magnitude and opposite in sign chirp to the pump and Stokes fields.

IV. NONADIABATIC EFFECTS INDUCED BY THE COUPLING BETWEEN TWO-LEVEL SYSTEMS

Naturally, the Raman-active vibrational modes get coupled via external fields when pulses strike the molecules. When modeled, the coupling is fulfilled by the effective Rabi frequency Ω_3, the strength of which is determined, in particular, by the excitation fields [15]. Studying the effects of coupling may play an important role in interpreting the results observed in the laboratory. Most of the time, constraints are imposed on the coupling, implying weak dipole transition moments between specific states. However, in our studies, we have taken the most general approach where all the transitions are allowed (i.e., all four states are coupled to each other through the fields). Figure 7 shows the exact solution obtained by solving the Schrödinger equation with the Hamiltonian in Eq. (3) for the two coupled TLSs using the Runge-Kutta method [10]. The final population of the excited state of the detuned TLS is nearly 60% and that of the excited state of the resonant TLS is nearly 20%. It can be implied from the comparison with the previous results that the coupling between the modes has induced nonadiabatic effects in the system and has resulted in the mixed population distribution among the TLSs.

To gain more insight into the physics behind the evolution of the systems and the nonadiabaticity induced by the coupling, we performed a dressed-state analysis. By diagonalization

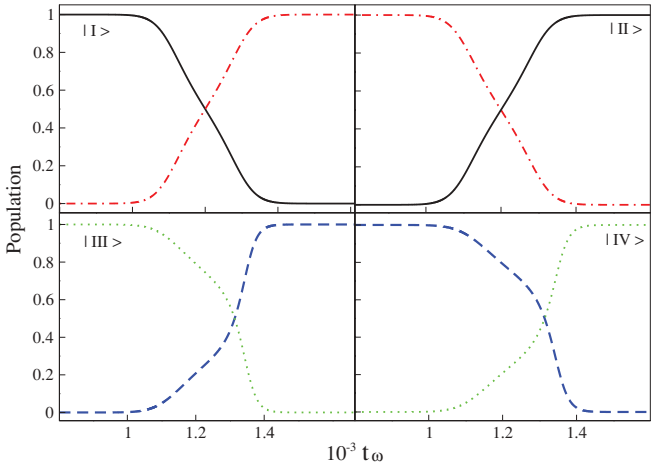

FIG. 6. (Color online) Population dynamics of bare states within the four different dressed states is shown in four inserts for parameters $\alpha'/\tau_0^2 = 10$ and a peak pulse intensity of 2×10^{12} W/cm^2. Black (solid), red (dot dashed), green (dotted), and blue (dashed) curves show population of the bare states $|1\rangle$, $|2\rangle$, $|3\rangle$, and $|4\rangle$, respectively.

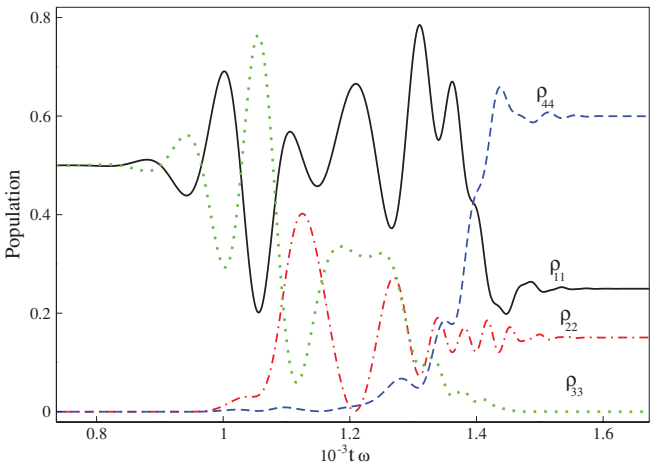

FIG. 7. (Color online) The population dynamics for two coupled TLSs as a function of time for parameters $\alpha'/\tau_0^2 = 10$ and a peak pulse intensity of 2×10^{12} W/cm^2. Black (solid), red (dot dashed), green (dotted), and blue (dashed) curves represent populations of states $|1\rangle$, $|2\rangle$, $|3\rangle$, and $|4\rangle$, respectively.

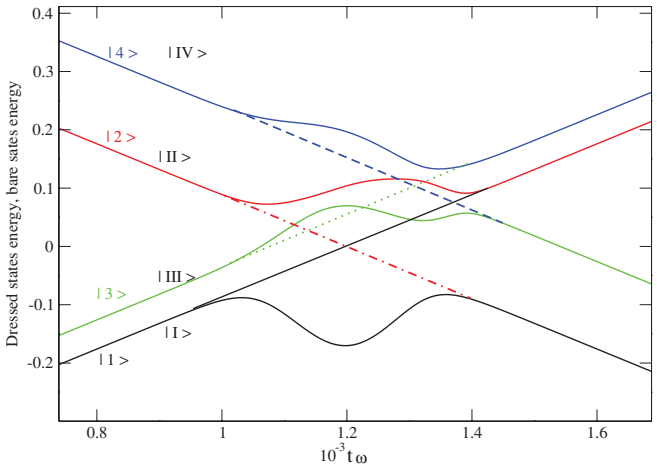

FIG. 8. (Color online) Time-dependent picture of the energies of the dressed states I, II, III, and IV for two coupled TLSs and the energies of the bare states (dashed lines) as a function of time for parameters $\alpha'/\tau_0^2 = 10$ and a peak pulse intensity of 2×10^{12} W/cm^2.

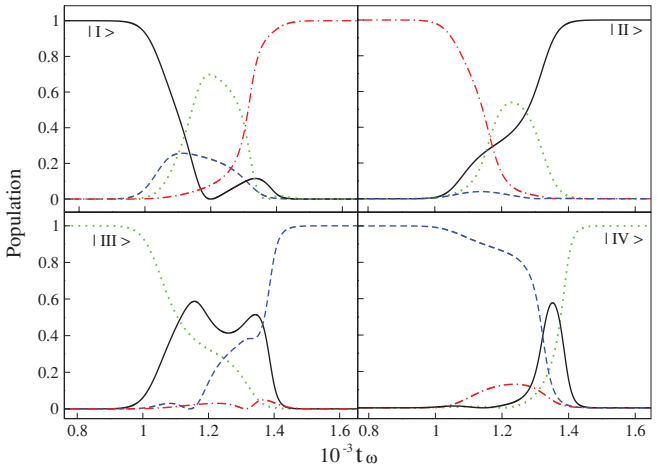

FIG. 9. (Color online) Population dynamics in the bare states within four different dressed states is shown in four inserts for parameters $\alpha'/\tau_0^2 = 10$ and a peak pulse intensity of 2×10^{12} W/cm^2. Black (solid), red (dot dashed), green (dotted), and blue (dashed) curves show the time evolution of population of bare states $|1\rangle$, $|2\rangle$, $|3\rangle$, and $|4\rangle$, respectively.

of the Hamiltonian in Eq. (3), we obtained the dressed-state energies presented in Fig. 8. We observe two avoiding crossings between different dressed states. They are placed very close and are relatively narrow, providing population flow from one dressed state to another. Initially, dressed states I and III are populated due to their coincidence with the energy of the bare states $|1\rangle$ and $|3\rangle$. As both the pump and Stokes pulses evolve in time, the energy of dressed states II and III approach one avoiding crossing that is followed by another avoiding crossing for states II and IV. These two avoiding crossings are not really separated in time, so they cannot be considered independently. Such a complex picture results in essentially nonadiabatic population transfer between all the dressed states. It implies that, by including the coupling in the system, we loose control over Raman transitions and are unable to obtain a population inversion in the modes. Population dynamics between the bare states within each of four dressed states is shown in Fig. 9. For the dressed states I and III, the population inversion is observed in the resonant and detuned TLSs, respectively. However, in the Schrödinger picture, owing to the nonadiabatic nature of light-matter interaction, all the dressed states are mixed and the population inversion is not reachable, as is seen in Fig. 7. Thus, the coupling between the modes leads to nonadiabaticity. However, a possibility of an efficient population transfer may exist if to apply suitably delayed pulses as it was first fulfilled by Oreg, Hioe, and Eberly [16]. Their method was realized experimentally by Gaubatz *et al.* [17] and many others. In this approach, controlling the pulse delay between the pump and Stokes pulses leads to the desired population inversion in both TLSs. Introducing the time delay between the pulses separates the dynamics in the coupled TLSs. It was shown by Gaubatz that the lowest losses from nonadiabatic coupling between the states are achieved when the delay is equal to the pulse bandwidth.

Following this approach, we introduced the 100-fs time delay between the Stokes pulse and the pump pulse, with the Stokes pulse running first. This pulse sequence resembles the stimulated Raman adiabatic passage (STIRAP) scheme. We have seen earlier that the crossing between the bare-state populations in the detuned TLS occurs after the central time. Now that we have introduced the time delay, the crossing will occur further away from the central time associated with the Stokes pulse. Control over the population dynamics is achieved by the two frequency components arising in the continuously changing beat frequency of the chirped pump and Stokes pulses. The lower-frequency component leads the higher-frequency component. This inverts the resonant TLS first since the transition frequency of this TLS is lower than that of the detuned TLS. After a 100-fs time delay, the detuned TLS gets inverted. At this time the lower-frequency vibrational mode is already inverted

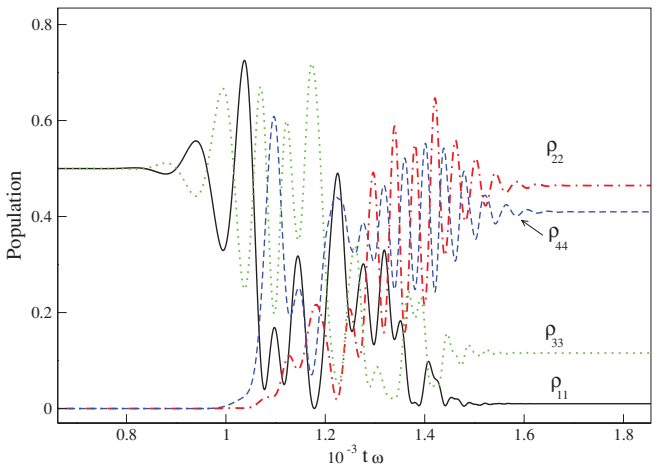

FIG. 10. (Color online) Population dynamics in two coupled TLSs as a function of time for parameters $\alpha'/\tau_0^2 = 10$, a 100-fs time delay between the Stokes and pump pulses, and a peak pulse intensity of 2×10^{12} W/cm^2. The black (solid), red (dot dashed), green (dotted), and blue (dashed) curves represent populations of the bare states $|1\rangle$, $|2\rangle$, $|3\rangle$, and $|4\rangle$, respectively.

and there will be no transition possible. Thus, we observe a population inversion in both TLSs in the presence of the coupling between them. Figure 10 shows the exact solution of population dynamics in the two coupled TLSs.

V. CONCLUSION

We have discussed a theory of the interaction between the chirped pump and Stokes laser pulses with vibrational modes with the goal to reveal the effect of the coupling between modes via external fields on the population dynamics and to explore a possibility for population inversion under these conditions. We have examined the effects of coupling by studying two cases: first, when the coupling between the modes is zero and, second, when the coupling is switched on. The two uncoupled TLSs give a robust population inversion in the resonant and detuned TLSs. However, in two coupled TLSs, a mixed distribution of population is observed owing to the nonadiabatic nature of the pump- and Stokes-pulse interaction with molecules. The performed dressed-state analysis revealed a possibility for strong nonadiabatic effects in this case. Upon exploring the coherent control mechanisms of light-matter interaction, we found that, by adding the time delay between the pump and Stokes pulse, one can achieve the desired population inversion in both coupled vibrational modes. The exact solution with the pump pulse delayed by 100 fs shows nearly complete population inversion in both coupled TLSs.

ACKNOWLEDGMENTS

The authors acknowledge fruitful discussions with Prof. V. S. Malinovsky and partial financial support from DARPA HR0011-09-1-0008 and NSF PHY-0855391.

[1] P. R. Berman and V. S. Malinovsky, *Principles of Laser Spectroscopy and Quantum Optics* (Princeton University Press, Princeton, 2010).
[2] V. S. Malinovsky and J. L. Krause, Phys. Rev. A **63**, 043415 (2001).
[3] J. Cao, C. J. Bardeen, and K. R. Wilson, J. Chem. Phys. **113**, 1898 (2000).
[4] K. Bergmann, H. Theuer, and B. W. Shore, Rev. Mod. Phys. **70**, 1003 (1998).
[5] M. N. Kobrak and S. A. Rice, Phys. Rev. A **57**, 1158 (1998).
[6] H. S. Moon, H. A. Kim, J. B. Kim, A. S. Choe, and J. L. Lee, J. Phys. B At. Mol. Opt. Phys. **32**, 987 (1999).
[7] B. Amstrup, A. Lorincz, and S. A. Rice, J. Phys. Chem. **97**, 6175 (1993).
[8] S. Ruhman and R. Kosloff, J. Opt. Soc. Am. B **7**, 1748 (1990).
[9] G. Cerullo, C. J. Bardeen, Q. Wang, and C. V. Shank, Chem. Phys. Lett. **262**, 362 (1996).
[10] W. H. Press, W. T. Vetterling, S. A. Tuekolsky, and B. P. Flannery, *Numerical Recipes in Fortran 77: The Art of Scientific Computing* (Cambridge University Press, Cambridge, 2001).
[11] T. C. Weinacht, J. L. White, and P. H. Bucksbaum, J. Phys. Chem. A **103**, 10166 (1999).
[12] B. J. Pearson, J. L. White, T. C. Weinacht, and P. H. Bucksbaum, Phys. Rev. A **63**, 063412 (2001).
[13] S. A. Malinovskaya, P. H. Bucksbaum, and P. R. Berman, Phys. Rev. A **69**, 013801 (2004).
[14] C. L. Evans, E. O. Potma, M. Puoris'haag, D. Cote, C. P. Lin, and X. S. Xie, PNAS **102**, 16807 (2005).
[15] V. Patel, V. S. Malinovsky, and S. A. Malinovskaya, Phys. Rev. A **81**, 063404 (2010).
[16] J. Oreg, F. T. Hioe, and J. H. Eberly, Phys. Rev. A **29**, 690 (1984).
[17] U. Gaubatz, P. Rudecki, S. Schiemann, and K. Bergmann, J. Chem. Phys. **92**, 5363 (1990).